Thrust faults and the global contraction of Mercury

Thomas R. Watters
Center for Earth and Planetary Studies, National Air and Space Museum, Smithsonian Institution, Washington, D.C., USA

Mark S. Robinson
Center for Planetary Sciences, Northwestern University, Evanston, Illinois, USA

Craig R. Bina
Department of Geological Sciences, Northwestern University, Evanston, Illinois, USA

Paul D. Spudis
The Johns Hopkins University Applied Physics Laboratory, Laurel, Maryland, USA

Received 26 November 2003; accepted 22 December 2003; published 18 February 2004.

[1] Lobate scarps on Mercury are the surface expression of thrust faults and are generally thought to be the result of global contraction. Our analysis indicates that these thrust faults are not uniformly distributed and exhibit non-random patterns on the imaged hemisphere. The greatest area normalized cumulative length of the faults occurs in the southern hemisphere, below 50°S. The thrust faults in this region dip to the north, indicating a broad zone where the crust has been displaced to the south. Widespread thrust faulting may not have initiated before the emplacement of Calorian smooth plains, well after the emplacement of pre-Tolstojan intercrater plains. Our observations suggest that regional-scale tectonic stresses on Mercury dominated over stresses resulting from global contraction. *INDEX TERMS:* 5430 Planetology: Solid Surface Planets: Interiors (8147); 5460 Planetology: Solid Surface Planets: Physical properties of materials; 5464 Planetology: Solid Surface Planets: Remote sensing; 5475 Planetology: Solid Surface Planets: Tectonics (8149); 6235 Planetology: Solar System Objects: Mercury. **Citation:** Watters, T. R., M. S. Robinson, C. R. Bina, and P. D. Spudis (2004), Thrust faults and the global contraction of Mercury, *Geophys. Res. Lett.*, *31*, L04701, doi:10.1029/2003GL019171.

1. Introduction

[2] Lobate scarps are linear or arcuate features that vary in relief from hundreds of meters to over a kilometer [*Watters et al.*, 1998, 2001], and range in length from tens to hundreds of kilometers [*Strom et al.*, 1975; *Cordell and Strom*, 1977]. Offsets in crater wall and floor materials transected by lobate scarps suggest they are the expression of surface breaking thrust faults (Figure 1) [*Strom et al.*, 1975; *Cordell and Strom*, 1977; *Melosh and McKinnon*, 1988; *Watters et al.*, 1998, 2001]. Forward mechanical modeling of Discovery Rupes, the largest of the known lobate scarps, suggests the thrust faults have a planar geometry [*Watters et al.*, 2002]. High-relief ridges are a less common tectonic landform on Mercury. They may have more than a kilometer of relief and are interpreted to be the surface expression of high-angle reverse faults (Figure 1) [*Watters et al.*, 2001].

0094-8276/04/2003GL019171$05.00

[3] The spatial and azimuthal distribution of lobate scarps on Mercury have been used to constrain thermal history models and models for the origin of tectonic stresses [see *Melosh and McKinnon*, 1988]. The most generally accepted model for the origin of the lobate scarp thrust faults is global contraction. Cooling of the interior and lithosphere results in significant thermal stresses [*Solomon*, 1976, 1978] that are compressional and horizontally isotropic. In a mechanically homogeneous lithosphere, such a stress state should result in uniformly distributed thrust faults in a random pattern with no preferred orientation or preferred fault plane dip direction [see *Watters et al.*, 2001].

2. Mapping Results

[4] Eighty-two lobate scarps and eight high-relief ridges were digitized directly from Mariner 10 image mosaics (Figure 2) with improved radiometry and geometric rectification [*Robinson et al.*, 1999]. Topographic data derived from Mariner 10 stereo coverage was also used where available [*Watters et al.*, 1998, 2001, 2002]. Lobate scarp were identified on the basis of evidence of vertical offset of the plains material and vertical offset of transected impact crater walls and floors. High-relief ridges were identified from evidence of uplift of transected impact craters, or association with lobate scarps (i.e., lobate scarps - high-relief ridge transition). The areal extent of the features was also considered. In particular, landforms that appear to offset the floors of impact craters but do not extend into or beyond the crater walls were not included. The tectonic features were divided into segments on the basis of orientation, with lengths generally >5 km. The locations of over 450 segments have been digitized and coded according to the structure-type.

3. Spatial and Temporal Distribution

[5] The spatial distribution of the tectonic features was analyzed by plotting their cumulative length in 20° latitude bins, normalized by area (Figure 3). Over 50% of the area normalized cumulative length of the tectonic features occurs below 30°S, with the greatest cumulative length between 50°S to 90°S (Figure 3). The largest lobate scarps on the imaged hemisphere (e.g., Discovery Rupes, Adventure

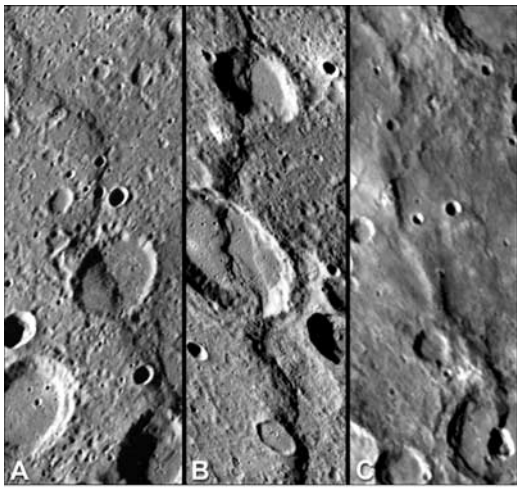

Figure 1. Prominent lobate scarps and a high-relief ridge on Mercury. Santa Maria Rupes (A) and Discovery Rupes (B) are lobate scarps formed by surface breaking thrust faults, and Antoniadi Dorsa (C) is a high-relief ridge formed by a blind (non-surface breaking) high-angle reverse fault. A and B are ~65 km across, and C is ~140 km across.

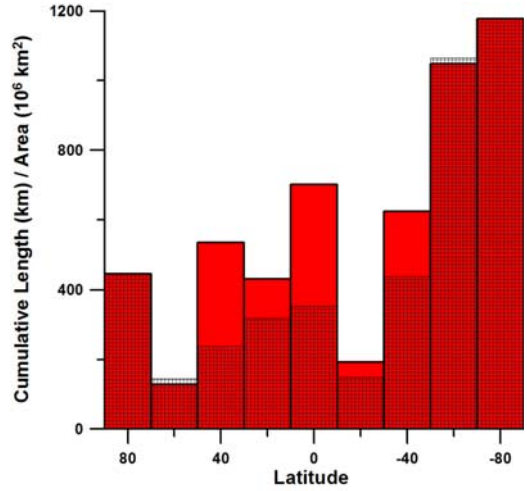

Figure 3. Spatial distribution of lobate scarps and high-relief ridges on Mercury as a function of latitude. The distribution of all the lobate scarps and high-relief ridges in the imaged hemisphere (patterned) and only the lobate scarps and high-relief ridges beyond 50° of the subsolar point (red) are shown. The cumulative length of digitized segments is area normalized.

Rupes, Hero Rupes) occur in this region. In the northern hemisphere, there is a gradual decrease in the area normalized cumulative length from the equator toward higher latitudes, with the exception of the north polar region (70°N to 90°N) (Figure 3).

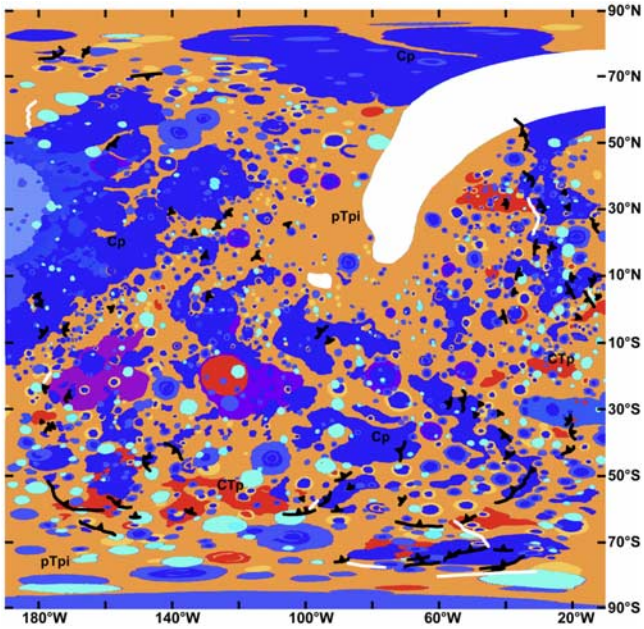

Figure 2. Location of lobate scarps and high-relief ridges on Mercury. Digitized segments of lobate scarps (black) and high-relief ridges (white) are overlaid on the geologic map of Mercury [*Spudis and Guest*, 1988]. The major geologic units are intercrater plains material pTpi (tan), Calorian-Tolstojan plains material CTp (red), and Calorian plains material Cp (blue). The dip directions of thrust faults are indicated by black triangles.

[6] The distribution of tectonic features may be influenced by observational bias caused by variations in lighting geometry across the imaged hemisphere. The incidence angle varies from 90° at the terminator to 0° at the subsolar point (0°N, 100°W). Thus, only a small percentage of the hemisphere imaged by Mariner 10 has an optimum lighting geometry for the identification of morphologic features. Many of the mapped tectonic features (~82%) occur where the incidence angle is >50° (~40° from the terminator) (Figure 2), suggesting that the apparent distribution of tectonic features may be skewed. Also, the number of lobate scarps near the subsolar point is much less than the number mapped where the incidence angle is >50° (Figure 2). This may indicate that many lobate scarps near the subsolar point remain undetected or that there are simply fewer structures in this region. To determine the possible effects of observational bias on the spatial distribution, that portion of the surface within 50° of the subsolar point was eliminated and the corresponding area subtracted from the area normalized cumulative length plots (Figure 3). Although eliminating the lobate scarps within 50° of the subsolar point (leaving a survey area of ~23% of the surface) does increase their cumulative length at the equator and in the northern mid-latitudes, the distribution of the remaining scarps is far from uniform (Figure 3). This analysis also suggests that the structures are not uniformly distributed even in the areas were the illumination geometry is the most favorable (incidence angle >50°).

[7] *Cordell and Strom* [1977] first noted the orientations of most lobate scarps are between ±45° of north. They attributed this preferred orientation to observational bias due to lighting geometry [see *Melosh and McKinnon*, 1988]. A plot of length-weighted azimuths of the digitized segments indicates that there is a strong preferred orientation (Figure 4). The majority of the segments have orientations that fall between ±50° of north-south (mean vector ~N12°E, circular variance ~0.72). Eliminating the

lobate scarps within 50° of the subsolar point (Figure 4) does not significantly change the distribution of orientations or the mean vector (~N7°E for remaining lobate scarps).

[8] To determine if the orientations of the mapped lobate scarps are from a population with a uniform distribution (i.e., random), we used Kuiper's Test [*Fisher*, 1993]. The Kuiper's V statistic, which is based on the largest vertical deviations above and below the diagonal line representing a uniform distribution, is ~25. Based on this large deviation, the hypothesis that the sample orientations are drawn from a uniform distribution is rejected. The deviation from a uniform distribution is illustrated in a uniformity plot of the orientations (see auxiliary Figure[1]).

[9] The preferred enhancement of features oriented perpendicular to the local illumination direction may also introduce an observational bias [*Melosh and McKinnon*, 1988; *Thomas et al.*, 1988]. Many of the tectonic features appear to be broadly concentric to the subsolar point (Figure 2). However, an analysis of the concentration of intersections of great circles fit to the perpendiculars of scarp segments [see *Watters et al.*, 2001] indicates only a weak correlation with the subsolar point (<2.5% of intersections of great circles).

[10] Lobate scarps and high relief ridges occur in pre-Tolstojan intercrater plains and Tolstojan and Calorian smooth plains units (Figure 2) [see *Spudis and Guest*, 1988]. Although the oldest deformed units are the pre-Tolstojan intercrater plains [*Strom et al.*, 1975; *Melosh and McKinnon*, 1988; *Watters et al.*, 2001], the lobate scarps appear to be much younger than these plains materials. Younger Tolstojan and Calorian aged smooth plains overlay intercrater plains (Figure 2), estimated to cover up to ~40% of the hemisphere imaged by Mariner 10 [*Spudis and Guest*, 1988]. If these structures formed only in the older intercrater plains, their distribution would be influenced by the areal extent of smooth plains (by burial). However, scarps are also found in both Tolstojan and Calorian aged smooth plains units (Figure 2), including the smooth plains surrounding the Caloris basin (35°N, 185°W) where the dominant tectonic features are wrinkle ridges. No evidence of embayment of lobate scarps by Tolstojan and Calorian smooth plains materials has been found. Also, while lobate scarps and high-relief ridges often deform impact craters, some as large as 60 km in diameter (Figure 1), there are no examples of large impact craters superimposed on these structures. These observations suggest that the structures are younger than the youngest endogenic unit on the planet (Calorian smooth plains). Another line of evidence suggesting a relatively young age for the lobate scarps and high-relief ridges is the absence of significant degradation or partial burial of the structures in the northern hemisphere by Caloris ejecta. Structures in intercrater plains adjacent to the Caloris Basin appear as well preserved as those formed in the surrounding Calorian smooth plains.

[11] The dip directions of the thrust faults inferred from the hanging wall-foot wall relationship (i.e., direction of vergence of the scarp faces) was also analyzed. In the northeastern part of the imaged hemisphere (~30°N, 30°W), N-S trending lobate scarps exhibit dips to the east and west (Figure 2). However, in the southern hemisphere, below 50°S, the lobate scarp thrust faults all dip to the north, NW, or NE; none dip to the south (Figure 2). In this broad zone across the hemisphere, the crust has been displaced to the south.

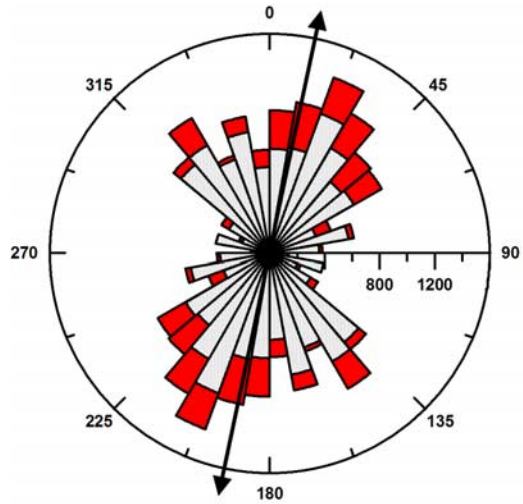

Figure 4. Rose diagram showing the distribution of orientations of lobate scarps and high-relief ridges. The distribution in orientations of all the lobate scarps and high-relief ridges in the imaged hemisphere is shown in red (mean vector, indicated by black arrow, is ~N12°E with a circular variance of 0.72) and the distribution of only those structures beyond 50° of the subsolar point is shown in gray (pattern). Orientations are length weighted by dividing segments of constant orientation into 1 km intervals. The horizontal axis is in units of kilometers.

[12] Examination of the relationship between the lobate scarps and regional topography in the southern hemisphere suggests that some of the structures were localized by mechanical discontinuities introduced by the rims and rings of ancient buried impact basins. Three lobate scarps, Discovery Rupes (~53°S, 35°W), Astrolabe Rupes (~41°S, 70°W), and Mirni Rupes (~37°S, 40°W) appear to be concentric to a previously unrecognized ancient basin about 550 km in diameter (centered ~43°S, 54°W) revealed by topographic data [*Watters et al.*, 2001]. Topographic data suggests that other prominent lobate scarps such as Hero Rupes (~59°S, 172°W) and Fram Rupes (~58°S, 94°W) may also be associated with an ancient impact basin. Many of the basins tentatively identified with the topographic data correspond to previously mapped pre-Tolstojan multiring basins identified solely on the basis of remnant massifs and arcuate patterns of tectonic features [*Spudis and Guest*, 1988]. Two other previously unrecognized buried impact basins (centered ~45°S, 142°W and ~10°N, 17°W) about 300 km in diameter are suggested by two opposite-facing arcuate lobate scarps that ring topographic depressions.

4. Implications and Discussion

[13] Our results suggest that the thrust faults in the hemisphere imaged by Mariner 10 are not spatially random.

[1]Auxiliary material is available at ftp://ftp.agu.org/apend/gl/2003GL019171.

Additionally, the temporal distribution of the faults suggests they may have all formed after the emplacement of Calorian smooth plains (<3.9 Gyr ago). Thermal history models predict slow thermal contraction of the planet with the greatest contraction occurring in the lithosphere [*Solomon*, 1976]. The models also predict that some lithospheric contraction would occur before the end of the period of heavy bombardment [*Solomon*, 1977; *Schubert et al.*, 1988]. If widespread thrust faulting initiated prior to the end heavy bombardment, evidence of partially buried or obliterated lobate scarps formed in pre-Tolstojan intercrater plains would be expected. The lack of such evidence suggests that either the bulk of the thermal contraction occurred before the emplacement of intercrater plains (pre-4.0 Gyr) or that compressional stresses from thermal contraction were not sufficient to initiate large-scale thrust faulting after the emplacement of intercrater plains. An important constraint on the state of stress in the lithosphere at the time the thrust faults formed is the absence of extensional features in intercrater or smooth plains (excluding the interior plains of the Caloris Basin). The lack of extensional features in these plains materials indicates a global compressional bias still existed when the thrust faults formed. Since the lithosphere is much weaker in tension than compression, post heavy bombardment global contraction related stresses may have been sufficient to retard the formation of extensional features. If this was the case, the lobate scarp thrust faults may be the result of a combination of regional-scale compressional stresses and stresses from global thermal contraction. Large-scale mechanical anisotropies must have also strongly influenced the formation of many lobate scarps. Ancient buried impact basins and zones of weakness created by very early crustal deformation (before the end of the period of heavy bombardment) may be reflected in the patterns of the observed thrust faults.

[14] Regional-scale stresses in smooth plains on Mercury may be due to subsidence. Topographic data indicate that the smooth plains of Tir Planitia (~0°N, 180°W), where several lobate scarps and numerous wrinkle ridges occur, are in a broad depression more than 1 km below the adjacent intercrater plains [*Harmon et al.*, 1986]. Outside of smooth plains, however, subsidence may not have been significant. Regional patterns of crustal displacement expressed by the lobate scarps may suggest other sources of stress. In the most heavily deformed region on the imaged hemisphere, below 50°S, the lobate scarp faults have generally southward thrust slip directions. These faults occur in a zone that extends over 3,000 km (Figure 2). On Earth, deformation zones consisting of thrust faults with a common slip direction are found in fold and thrust belts located at convergent plate margins. Although on a one-plate planet analogous terrestrial plate motions are ruled out, tectonic stresses may have been induced by convective motion in Mercury's mantle. Modeling shows that mantle convection on Mercury was likely in a stagnant lid regime [*Solomatov and Moresi*, 1997, 2000], and may still exist beneath Mercury's lithosphere [*Schubert et al.*, 1988]. Modeling suggests that the effective elastic thickness T_e of the lithosphere at the time of faulting was ~25 to 30 km [*Nimmo and Watters*, 2004], possibly thin enough to have been influenced by stresses induced by mantle convection. However, the small size of Mercury's mantle, perhaps no more then ~500 km thick at time of lobate scarp formation, may have limited the length-scale of mantle driven tectonism. Another possibility is stress induced by downwelling in Mercury's upper mantle. On Earth, intraplate compression may result from downwelling of dense upper mantle material due to a gravitational instability (Rayleigh-Taylor) that transmits shear stresses to the base of the crust, causing crustal thickening [*Neil and Houseman*, 1999]. If a similar mechanism occurred on Mercury, thrust faulting may be associated with regions of greater crustal thickness. Ultimately, imaging and topographic data to be returned by the MESSENGER mission [*Solomon et al.*, 2001] will make a global analysis of Mercury's tectonic features possible.

[15] **Acknowledgments.** We thank Robert G. Strom and an anonymous reviewer for their helpful reviews. This research was supported by grants from National Aeronautics and Space Administration's Planetary Geology and Geophysics Program.

References

Cordell, B. M., and R. G. Strom (1977), Global tectonics of Mercury and the Moon, *Phys. Earth Planet. Inter.*, *15*, 146.

Fisher, N. I. (1993), *Statistical Analysis of Circular Data*, 277 pp., Cambridge Univ. Press, Cambridge.

Harmon, J. K., D. B. Campbell, K. L. Bindschadler, J. W. Head, and I. I. Shapiro (1986), Radar altimetry of Mercury: A preliminary analysis, *J. Geophys. Res.*, *91*, 385–401.

Melosh, H. J., and W. B. McKinnon (1988), The tectonics of Mercury, in *Mercury*, edited by F. Vilas, C. R. Chapman, and M. S. Matthews, pp. 374–400, University of Arizona Press, Tucson, AZ.

Neil, E. A., and G. A. Houseman (1999), Rayleigh-Taylor instability of the upper mantle and its role in intraplate orogeny, *Geophys. J. Int.*, *138*, 89–107.

Nimmo, F., and T. R. Watters (2004), Depth of faulting on Mercury: Implications for heat flux and crustal and effective elastic thickness, *Geophys. Res. Lett.*, *31*, L02701, doi:10.1029/2003GL018847.

Robinson, M. S., M. E. Davies, T. R. Colvin, and K. E. Edwards (1999), A revised control network for Mercury, *J. Geophys. Res.*, *104*, 30,847–30,852.

Schubert, G., M. N. Ross, D. J. Stevenson, and T. Spohn (1988), in *Mercury*, edited by F. Vilas, C. R. Chapman, and M. S. Matthews, pp. 429–460, University of Arizona Press, Tucson, AZ.

Spudis, P. D., and J. E. Guest (1988), Stratigraphy and geologic history of Mercury, in *Mercury*, edited by F. Vilas, C. R. Chapman, and M. S. Matthews, pp. 118–164, University of Arizona Press, Tucson, AZ.

Solomon, S. C. (1976), Some aspects of core formation in Mercury, *Icarus*, *28*, 509–521.

Solomon, S. C. (1977), The relationship between crustal tectonics and internal evolution in the Moon and Mercury, *Phys. Earth Planet. Inter.*, *15*, 135–145.

Solomon, S. C. (1978), On volcanism and thermal tectonics on one-plate planets, *Geophys. Res. Lett.*, *5*, 461–464.

Solomon, S. C., et al. (2001), The MESSENGER Mission to Mercury: Scientific Objectives and Implementation, *Planet. Space Sci.*, *49*, 1445–1465.

Solomatov, V. S., and L.-N. Moresi (1997), Three regimes of mantle convection with non-Newtonian viscosity and stagnant lid convection on the terrestrial planets, *Geophys. Res. Lett.*, *24*(15), 1907–1910.

Solomatov, V. S., and L.-N. Moresi (2000), Scaling of time-dependent stagnant lid convection: Application to small-scale convection on Earth and other terrestrial planets, *J. Geophys. Res.*, *105*(B9), 21,795–21,818.

Strom, R. G., N. J. Trask, and J. E. Guest (1975), Tectonism and volcanism on Mercury, *J. Geophys. Res.*, *80*, 2478–2507.

Thomas, P. G., P. Masson, and L. Fleitout (1988), Tectonic history of Mercury, in *Mercury*, edited by F. Vilas, C. R. Chapman, and M. S. Matthews, pp. 401–428, University of Arizona Press, Tucson, AZ.

Watters, T. R., M. S. Robinson, and A. C. Cook (1998), Topography of lobate scarps on Mercury: New constraints on the planet's contraction, *Geology*, *26*, 991–994.

Watters, T. R., M. S. Robinson, and A. C. Cook (2001), Large-scale lobate scarps in the southern hemisphere of Mercury, *Planet. Space Sci.*, *49*, 1523–1530.

Watters, T. R., R. A. Schultz, M. S. Robinson, and A. C. Cook (2002), The mechanical and thermal structure of Mercury's early lithosphere, *Geophys. Res. Lett.*, *29*(11), 1542, doi:10.1029/2001GL014308.

C. R. Bina, Department of Geological Sciences, Northwestern University, Evanston, IL 60208, USA.

M. S. Robinson, Center for Planetary Sciences, Northwestern University, Evanston, IL 60208, USA.

P. D. Spudis, The Johns Hopkins University Applied Physics Laboratory, Laurel, MD 20723, USA.

T. R. Watters, Center for Earth and Planetary Studies, National Air and Space Museum, Smithsonian Institution, Washington, D.C. 20560, USA. (twatters@nasm.si.edu)